Video-Rate Switching of High-Reflectivity Hybrid Cavities Spanning All Primary Colors

ADVANCED MATERIALS
www.advmat.de

Video-Rate Switching of High-Reflectivity Hybrid Cavities Spanning All Primary Colors

Kunli Xiong, Oliver Olsson, Stefano Rossi, Gan Wang, Magnus P. Jonsson, Andreas Dahlin, and Jeremy J. Baumberg*

Dynamically tunable reflective structural colors are attractive for reflective displays (electronic paper). However, it is challenging to tune a thin layer of structural color across the full red–green–blue (RGB) basis set of colors at video rates and with long-term stability. In this work, this is achieved through a hybrid cavity built from metal–insulator–metal (MIM) "nanocaves" and an electrochromic polymer (PProDOTMe$_2$). The reflective colors are modulated by electrochemically doping/dedoping the polymer. Compared with traditional subpixel-based systems, this hybrid structure provides high reflectivity (>40%) due to its "monopixel" nature and switches at video rates. The polymer bistability helps deliver ultralow power consumption (≈2.5 mW cm^{-2}) for video display applications and negligible consumption (≈3 µW cm^{-2}) for static images, compatible with fully photovoltaic powering. In addition, the color uniformity of the hybrid material is excellent (over cm^{-2}) and the scalable fabrication enables large-area production.

1. Introduction

Electronic displays have fundamentally revolutionized human interactivity, industrial production, and services over the past half-century. A drawback is their high energy consumption, which will further increase with the development of virtual reality technologies. Emissive displays based on light-emitting diodes (LED) or liquid crystals (LCD) have little room for further improvements in energy conversion efficiency and their power use becomes especially high in daylight.[1] The most energy-saving display technology is a reflective display (E-paper), which does not emit light but instead reflects ambient illumination as with ordinary printed paper, thus consuming little power.[2] In contrast to current emissive displays which are hard to view under sunshine, E-paper offers a glare-free display and provides excellent visibility in bright environments. In addition, the usage of E-paper has been found to improve circadian rhythm health compared to emissive displays.[3] However, most commercial E-paper (such as in Amazon Kindle) based on electrophoretic inks[4] (EPD) suffer from poor color quality and slow refresh rate (≈1 s). For the entire E-paper industry, high brightness (>40%) in color mode and video display capability (>24 Hz) are the two main challenges limiting the replacement of emissive displays. For E-paper, ambient light determines the maximum brightness so high color performance fundamentally requires a compromise between optimizing chromaticity and reflectivity.[5] As a result, using traditional RGB subpixels to display colors is unsuitable for E-paper since only a fraction of the subpixels (33% at best) are activated for each primary color,[6] significantly reducing the total reflectivity.

In order to enhance the total reflectivity, the development of tunable color pixels ("monopixels") is essential since they do not sacrifice the reflectance of subpixels to generate colors.[7] If a structure can switch between all three primary colors (i.e., red, green, and blue), it can cover the entire visible range, and eliminate the need for subpixels. One example is the electrowetting display,[8] which provides color monopixels covering the visible range at video-rate switching. This device superimposes three dyed microfluidic layers and individually modulates the optical transmittance of each layer to generate any color. However, due to the inevitable optical absorption from each electrochromic layer, their reflectivity is only ≈10%,[9] which prevents market acceptance even after 20 years of development. In recent years, various tunable color technologies using only a single electrochromic layer have been developed.[7,10,11,12,13] One type uses

K. Xiong, J. J. Baumberg
Nanophotonics Centre
Department of Physics
Cavendish Laboratory
University of Cambridge
Cambridge, England CB3 0HE, UK
E-mail: kunil@chalmers.se

K. Xiong, O. Olsson, A. Dahlin
Department of Chemistry and Chemical Engineering
Chalmers University of Technology
Gothenburg 41296, Sweden

K. Xiong, G. Wang
Department of Physics
University of Gothenburg
Göteborg 41296, Sweden

S. Rossi, M. P. Jonsson
Department of Science and Technology
Linköping University
Norrköping 60174, Sweden

The ORCID identification number(s) for the author(s) of this article can be found under https://doi.org/10.1002/adma.202302028

DOI: 10.1002/adma.202302028

polarization-dependent liquid crystals to control the reflective colors of an Al plasmonic nanomaterial.[11] However even here, the total reflectance is low since the polarizers attenuate incident light, and the switching speed is too slow (≈70 ms) for video display even at high operation voltages (50 V). Most recently, Rossi et al. showed a hybrid structure with the electroactive polymer PT34bT (poly-thieno[3,4-b]thiophene) between Au/Cr and Al layers.[12] The volume of PT34bT can be adjusted by electrochemical redox reactions, modulating the Fabry–Pérot mode to change the reflective colors across the visible. This material provides good chromaticity with high absolute reflectance but has poor color uniformity due to PT34bT thickness variations and angle dependence. Further issues are its few-second switching speed (far from video rate) and the device instability over more than 10 cycles, likely due to the fully organic cavity composition. In addition to effective color performance and video refresh rate (>24 fps), the commercial market also expects low operation voltage, relatively long lifetime, and color memory capability (so devices maintain color even without any power input). Existing E-paper technologies, including electrowetting displays,[14] tunable plasmonic resonances,[15] electrically responsive photonic crystals,[16] etc.,[17,18,19] cannot fulfill these requirements.

Here we present a dynamically tunable hybrid electrochromic nanostructure satisfying all the above requirements. To the best of our knowledge, it is the first material that uses only a single electrochromic layer to provide tunable reflective colors spanning all primary colors (RGB) with video switching capability. The monopixels provide high peak reflectivity (>40%), comparable to printed paper. We employ dimethylpropylenedioxythiophene ($PProDOTMe_2$) for its advantageous optical properties to modulate the reflective colors and provide video-rate switching speed (>33 fps) at low operation voltages ($-0.6 \leftrightarrow +0.75$ V). Moreover, the energy consumption of the hybrid material (≈2.5 mW cm^{-2}) is lower than the current most energy-saving E-papers (EPD ≈4.0 mW cm^{-2})[29] for video display, and has practically zero energy consumption (≈3 μW cm^{-2}) for static display because of its color memory (bistability) properties. Compared with using only polymers as the intracavity layer, the hybrid cavity improves the chromaticity of the system and also rigidifies the device geometry in the form of polymer-filled 'nanocaves', thus eliminating non-uniform color problems from thickness variation of the electrochemically deposited polymer. Similarly, the nanocaves improve the structural stability of the system compared with having only a polymer as spacer layer, greatly prolonging the device lifetime. Our work is capable of drastically improving the E-paper industry with significant potential for commercialization.

2. Results and Discussion

2.1. Fabrication of the Au-SiO_2-Pt (ASP) Nanocaves

The fabrication of the hybrid nanomaterial essentially contains two steps: preparing the Au-SiO_2-Pt (ASP) nanocaves, and then depositing the electrochromic polymer inside them. In brief, the ASP nanocaves work as a color generator, providing one of the primary colors. The electrochromic polymer modulates this color to reach the other two primary colors. Here, we choose $PProDOTMe_2$ as the electrochromic material because of its excellent optical (switching) properties, fast switching speed, low operating voltage, and ability to be selectively deposited on electrodes, e.g., only inside nanocaves.[20] The colors of the nanostructure are generated and modulated by Fabry–Pérot interference,[21] using the electrochromic material as the intracavity layer. This Fabry–Pérot interference arises from multiple reflection of light between two semi-reflective layers (**Figure 1**a), with the relative optical phase depending on effective refractive index and angle. Key to success is the hybrid nature of the cavity, which consists of both a solid material (SiO_2) for stability and a fast-switching electrochromic polymer that alters the permittivity in the nanocave. With suitable coverage of nanocaves and $PProDOTMe_2$, the modulated colors have access to all primary colors.

The basic structure of the ASP nanocaves (Figure 1a) is formed by a 1 nm Cr adhesion layer, a semitransparent 20 nm Au layer, a 175 nm SiO_2 spacer containing aperiodic studded nanocaves, and topped by a reflective mirror consisting of 40 nm Au, 40 nm Pt, and a 15 nm Al_2O_3 protective layers. When an observer looks from the glass side, the ASP structure generates a uniform reflective green color through Fabry–Pérot interference. The nanocaves formed as openings in the SiO_2 layer operate as capsules for accommodating $PProDOTMe_2$. Due to the high chemical stability and conductivity of Pt and Au, $PProDOTMe_2$ can be electrochemically deposited selectively inside the nanocaves. Additional Au "studs" (nanocylinders) increase the surface area of the electrode in the nanocaves, effectively reducing the thickness of $PProDOTMe_2$ for the same amount of polymer material, thereby increasing the modulation speed to video rates.[22] Finally, the Al_2O_3 protective layer prevents $PProDOTMe_2$ from growing outside the nanocaves, allowing us to precisely control the volume of internal $PProDOTMe_2$, and significantly reducing energy consumption during color modulation.

We prepare these nanostructures by combining established low-cost nanofabrication techniques (schematic of fabrication process in Figure S1, Supporting Information). Compared to our previous work,[22,23,24] we use here a "reversed" design that generates the reflective colors from the glass side. This design hides the electrolyte and counter-electrode behind the reflective colors, which improves the total reflectivity of real devices.[5] The short-range ordered 100 nm nanoholes (Figure 1b) formed by colloidal lithography allow the electrolyte to infiltrate into the nanocaves. The second Au evaporation forms studs at the base of each nanocave in the form of nanocylinders. Cross-sectional scanning electron microscopy (SEM) images (Figure 1b) confirm the presence of these studs, which increase the surface area of the bottom gold layer. Interestingly, while a significant part of the middle SiO_2 is seen to be etched out, the structure is robust and remains uncollapsed. Although hard to directly estimate from SEM images, the volume ratio of air to SiO_2 is estimated from simulating the reflection spectra during wet etching.

The nanocaves are formed by 0.08% hydrofluoric acid (HF) penetration through the nanoholes in the Pt mirror, which etches out the middle SiO_2 layer. With longer etching time (Figure 1c), the volume of each nanocave increases, leading to a higher volume ratio of air to SiO_2 and reducing the middle layer effective refractive index (RI). Due to Fabry–Pérot interference, the peak position of the reflectance thus blueshifts with decreasing average RI of the middle layer, in good agreement with the experimental results (Figure 1d). To compare changes in reflective color during wet etching, we fabricate aperiodic nanoholes only on the lower

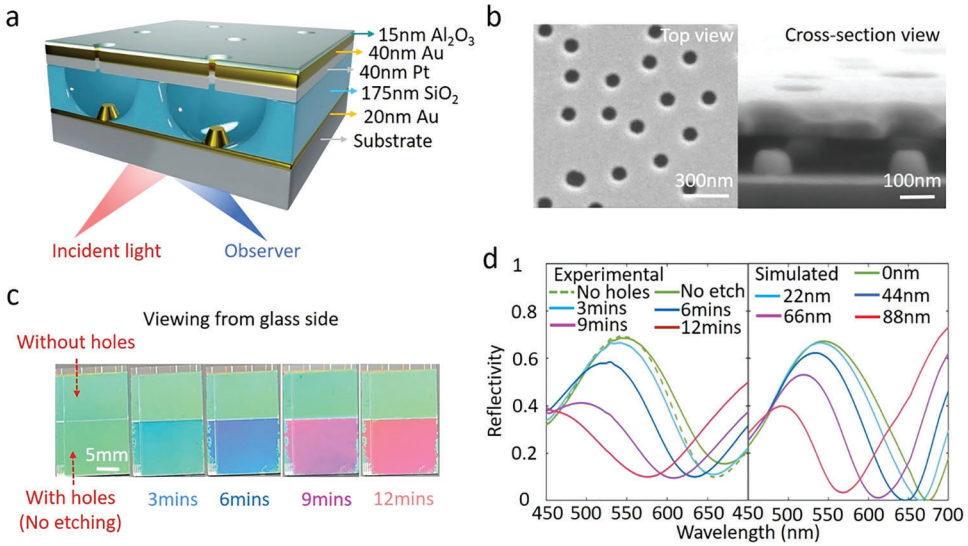

Figure 1. Nanostructure and optical properties. a) Schematic illustration of ASP nanocaves. Observers view colors from the glass substrate side. b) Electron microscopy images showing nanostructures in top- and cross-section views. c) Photos of sample (18 × 24 mm^2) with different etching times (as labeled). Lower side has nanocaves, while the upper side does not. d) Experimental and simulated reflectance spectra of ASP nanocaves for different etching times/ thickness of the air layer.

half of the sample. Its color changes from green through blue to red with increasing etch time (Figure 1c). Figure 1d shows calculated spectra based on the Fresnel equations for a multi-thin film system without the nanocaves (Figure S3a, Supporting Information), which differ only slightly from the experimental data. The experimental reflectance peak broadens for increasing etch times compared with the calculations, possibly due to scattering from the nanocavities and nanocylinders. However, the dip/peak positions fit the model well, implying that the etch rate is relatively stable over time and barely influenced by the nanocave structures (see Figure S2, Supporting Information for simulations of the full 3D structure with the nanocaves). When the volume ratio of air to SiO_2 is ≈1:1, the initially-green reflective color changes to red. If the wet etching is continued, the middle SiO_2 layer will not be stable enough to support the Pt mirror, leading to collapse and destroying the nanostructure (Figure S3d, Supporting Information). To verify the display performance of the nanomaterial, the Cambridge logo is reproduced by pixelating the nanomaterial, with a pixel size of 25 µm (Figure S9a, Supporting Information). The reflective colors change from red (air) to green (in propylene carbonate, PC). This shows that the electrolyte fills the internal void of the nanocaves, increasing the effective refractive index and causing a red shift in the reflective resonance peak. In addition, Fabry–Pérot interference is highly dependent on both the incident and observation angles. This can be seen when increasing reflection angles from 0° to 60° (Video S2, Supporting Information) for the PC-immersed sample where the reflective color changes from green to blue, caused by the decreasing optical phase difference.

2.2. Deposition of the $PProDOTMe_2$ in the ASP Nanocaves

After etching out the nanocaves, the next step is to deposit $PProDOTMe_2$ inside them and investigate the optical properties of the hybrid material. Our measurement setup (**Figure 2**a) tracks both polymerization charges and color modulation simultaneously by integrating an electrochemical fluidic cell with an optical microscope, recording reflection spectra through a low NA objective lens. The fluidic cell allows the exchange of electrolytes (without monomer) after every $PProDOTMe_2$ cyclic voltammetry (CV) deposition for color modulation measurements, to find the optimal polymer volume for best color performance. Electrochemical deposition is achieved in PC containing 0.1 M $LiClO_4$ and 0.01 M of the monomer.[22,25] The voltage on the working electrode linearly sweeps from −0.7 to +1.5 V at 200 mV s^{-1} relative to the reference electrode (Ag/AgCl). During testing, the electrolyte contains only $LiClO_4$ without monomer, and the voltage changes from −0.6 to 0.75 V. This activates the redox reaction of $PProDOTMe_2$ (Figure 2a bottom), doping ClO_4^- ions into the polymer during oxidation and changes its optical properties (but without further growing the film). The relation between the number of CV deposition cycles and the observed modulation colors (Figure 2b) shows changes in both gamut coverage and absolute reflectivity change. We emphasize that the colors within the gamut coverage would be generated by combining monopixels with different basis colors. Oxidizing $PProDOTMe_2$ increases the reflectivity in the blue-green region (450–550 nm) (arrows Figure 2b) while decreasing it in the red region (600–660 nm), and conversely in the reduction cycle. In the CIE diagram, the colors redshift for more deposition cycles since the effective RI of the middle layer increases. In order to modulate across all RGB colors, the curve should move around the center (white point) of the CIE diagram. This is optimal for 12 CV deposition cycles.

To enhance the switching speed of the system to video rates, as in our previous work[22] the solvent is changed from PC to acetonitrile for reduced viscosity. Moreover, due to its lower RI, the acetonitrile leads to better chromaticity than with PC (red triangle in CIE diagram in Figure 2c). We compare the experimental

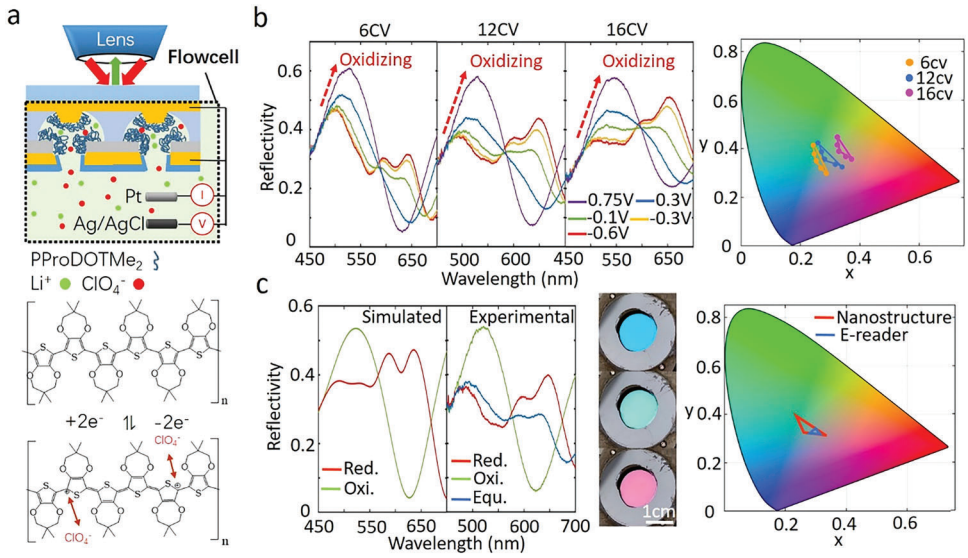

Figure 2. Dependence of number of CV deposition cycles on modulation color range. a) Schematic illustration of modulation setup and redox reactions of $PProDOTMe_2$. $PProDOTMe_2$ is electropolymerized and modulated by applied potential. Reflection is measured from the glass side. b) Reflectance spectra at five voltages for samples with increasing CV deposition cycles. The arrows indicate increases in green reflectance upon oxidation. Dots: gamut positions at different voltages. Lines: gamut coverages by hybridizing monopixels. c) Experimental and simulated reflectance spectra of hybrid nanocaves deposited with 12 CV cycles in different redox states. The photographs show 1.3 cm diameter samples in the redox states corresponding to the different spectra. The electrolyte is 1 M $LiClO_4$ in acetonitrile. Right: The gamut covered exceeds commercial E-reader colors (see text).

and simulated reflectance spectra of this hybrid nanomaterial in different redox states using acetonitrile as the electrolyte. This simulation model (Figure S4, Supporting Information) again uses Fresnel equations to calculate the multilayer reflectivity, with the permittivity of $PProDOTMe_2$ from literature.[26] Here, the tuning originates from controlling the permittivity of $PProDOTMe_2$ to adjust the reflective colors, while the intracavity layer thickness does not change since it is fixed by the SiO_2 nanocaves. Choosing materials with appropriate optical properties is essential, and $PProDOTMe_2$ meets current requirements for providing RGB reflective colors.

The real and imaginary RI ($\tilde{n}_2$) of $PProDOTMe_2$ in its different redox states is shown in Figure S4 (Supporting Information). In the oxidized state, the optical absorption ($\propto \mathrm{Im}\{\tilde{n}_2\}$) is low, giving reflectance spectra similar to conventional MIM cavities.[27] During reduction, the optical absorption significantly increases in the green wavelength range, leading to reflective color changes from green to blue. When further continuing the reduction, $\mathrm{Re}\{\tilde{n}_2\}$ significantly increases in the red. According to the complex-valued Snell's law,[28] for normal incident light the reflectivity of one thin layer is $\tilde{r} = \left|\frac{\tilde{r}_{12}+\tilde{r}_{23}e^{2i\beta}}{1+\tilde{r}_{12}\tilde{r}_{23}e^{2i\beta}}\right|^2$. Here, $\tilde{r}_{\mathrm{mn}} = \frac{\tilde{n}_{\mathrm{m}}-\tilde{n}_{\mathrm{n}}}{\tilde{n}_{\mathrm{m}}+\tilde{n}_{\mathrm{n}}}$, $\beta = (\frac{2\pi}{\lambda})\tilde{n}_2 h$, and h is the thickness of the middle layer. Although our structure has more than one thin film, this model can give an indication of what changes in reflectivity to expect from the gold film that the incident light hits first. For these hybrid nanocaves, $\tilde{n}_1$ corresponds to the RI of the Au layer. In the red, $\mathrm{Re}\{\tilde{n}_1\}$ is small (0.17 at 650 nm), and $\mathrm{Im}\{\tilde{n}_1\}$ is large (3.15 at 650 nm). During reduction, $\mathrm{Re}\{\tilde{n}_2\}$ significantly increases (1.3 → 2.1 at 650 nm), while $\mathrm{Im}\{\tilde{n}_2\}$ remains relatively small (0.17 → 0.3 at 650 nm) compared with Au. Thus, for the reduced state of $PProDOTMe_2$, $\tilde{r}_{12}$ in the red is closer to 1, increasing $\tilde{r}$ and changing the color from blue to red. Photographs of large area monopixels (Figure 2c) show the uniform reflective RGB colors of this hybrid material in different redox states, corresponding to the experimental spectra. For comparison, the color gamut of a commercial e-reader (PocketBook with E-Ink Kaleido released in 2020) is shown (blue triangle in Figure 2c).[5] The coverage of our hybrid nanomaterial is >400% larger than the e-reader (that also does not support video display). Our system thus provides high-quality chromaticity. In addition, we compare the Y values of the hybrid material with the E-reader (Figure S10, Supporting Information), revealing that the mean brightness value of the primary colors is about three times higher for the nanocaves compared to the e-reader. The next step involves implementing this hybrid nanomaterial on thin film transistor arrays for individual pixel addressing and polymer switching. The thin film transistor arrays replace the counter electrode and are hidden behind the reflective surface. To demonstrate the display performance of this hybrid nanomaterial, $PProDOTMe_2$ is deposited into nanocave pixels patterned in the Cambridge logo. The logo is electrochemically switched between red, green, and blue colors (Figure S9b, Supporting Information). The color performance is similar to the uniform colors shown in Figure 2c.

2.3. Fast Switching Colors

Accurately controlling the reflective colors with electrical signals is essential for practical applications to enable the hybrid nanomaterial to be integrated with thin-film transistor arrays. Due to the RI changes of $PProDOTMe_2$ with ion doping, the most direct method of modulating the reflective color is through applying different voltages (as shown in the previous section). The position and amplitude of the reflectance peak (**Figure 3**a) span the RGB colors when applying voltages from −0.6 to 0.7 V, with

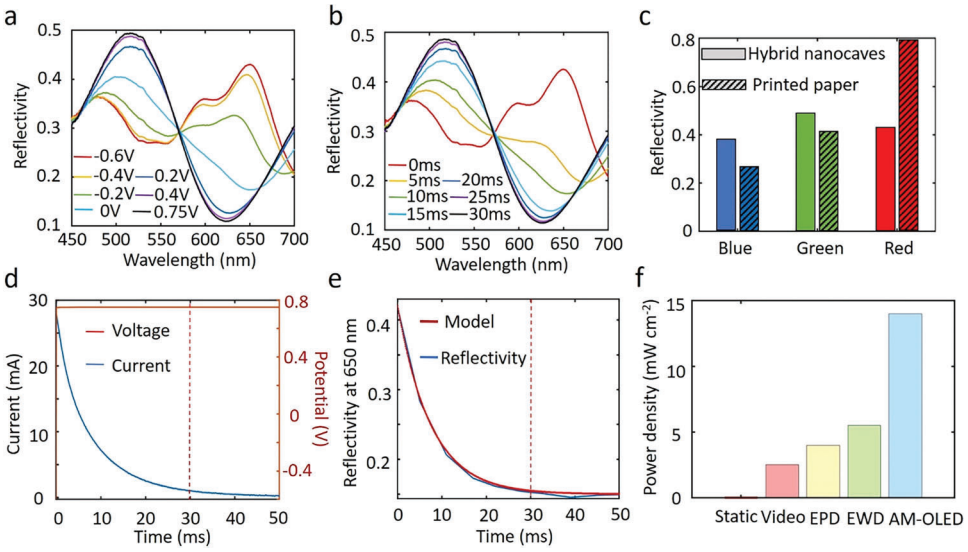

Figure 3. Modulating reflective colors by electrochemistry. a) Reflection spectra at different potentials. b) Reflection spectra for different pulse durations at 0.75 V. c) Peak reflectivities of hybrid nanocaves compared to printed paper across RGB colors. d) Switching dynamics of $R(t)$ as the voltage is reversed from −0.6 to 0.75 V. e) Reflectivity change at 650 nm vs time when color is modulated from red to green (blue line), with exponential fits to reflectivity and doping (red line). f) Power densities of hybrid nanocaves for static and video display (red), compared with average power use for black and white electrophoretic (EPD) displays, electrowetting (EWD) displays, and organic light-emitting diode (AM-OLED) displays.

the reduced hybrid material reflecting red color at negative voltage (Figure 2b). By increasing the voltage, the film changes to the oxidized state, leading to reflective colors first turning first blue and finally green. The RI variation and complex nanostructure give the peak reflectance that slightly varies for different colors: blue (485 nm) R≈38%, green (520 nm) R≈49%, and red (650 nm) R≈42%. To compare the color quality, we measure reflective spectra from ink spots produced by a laserjet printer on ordinary white paper (see Methods). The printed colors have relatively low peak reflectance in the blue (26%) and green (41%) but are higher in the red (77%) (Figure 3c) with a larger gamut coverage (Figure S5, Supporting Information). Future optimization of the synthesized polymer, including changes in monomer structure, should improve the chromaticity, particularly in the red.

We now demonstrate that the reflective colors can be accurately modified at fast switching speeds by adjusting the duration of a short voltage pulse. Importantly, in contrast with emissive displays (LCD, LED), this hybrid material keeps color even without putting in power, leading to its desired state being retained with short-duration pulses (non-continuous input signals). Initially, −0.6 V is applied to reduce the $PProDOTMe_2$ entirely (Figure 3b). Then, positive 0.75 V pulses of increasing duration are applied, generating reflectance spectra from red to green. The polymer is fully oxidized with a 30 ms duration pulse, giving a spectrum similar to the black line in Figure 3a. To further characterize the switching speed, we track the temporal variation of the current and reflectivity at 650 nm during the pulse (Figure 3d,e). More than 95% of the full switching occurs within 30 ms. Even though the polymer is inside nanocaves rather than on a flat surface, the reflected intensity (and current) simply changes exponentially, following first-order reaction kinetics (details in Figure S7, Supporting Information).

The change in reflected intensity tracks the redox state, which is modified by doping following the current flow, and follows the same exponential decay (Figure 3d,e). Applying a voltage pulse at $t = 0$, gives for $t > 0$, $I = I_0 \exp(-t/\tau)$ and $R = R_0 + R_a \exp(-t/\tau)$, with $R_0 = 15\%$, $R_a = 27\%$ at 650 nm. This assumes that the polymer layer is thin enough that absorption at different positions is not important. In this model, the characteristic time of the doping reaction is $\tau = 7.5$ ms (Figure 3e). For each full switch (from red to green, >95% intensity change), the charge transfer is $Q = \int I dt \approx 200$ μC in 30 ms. This reproducibility thus allows accurate control of the reflective color of these hybrid materials by metering electrical charge transferred (pulse duration). Compared to previous E-paper using $PProDOTMe_2$,[22] the energy consumption is further decreased since the new hybrid material needs even less polymer per area. With a charge density for each switch of ≃150 μC cm^{-2}, the maximum required current density operation at 33 Hz is only 5 mA cm^{-2}. The low average working voltages (0.75 V) translate to a total power density of 3.8 mW cm^{-2}. Moreover, the energy consumption for red to blue switching is even lower ≈1.7 mW cm^{-2}, since only shorter pulse durations of <5 ms are needed. Thus, the average energy consumption of the hybrid material is ≈2.5 mW cm^{-2}. The energy consumption for different electronic displays[29] (Figure 3f) shows the favorable performance of hybrid nanocaves. Even though the energy consumption of our system is seriously overestimated here since not all pixels change color during a video (typically <10% change per frame[30]), it is lower than the most energy-saving displays (EPD) since EPDs operate at >10 V.[31] We emphasize that EPDs (yellow bar in Figure 3f) do not support video display, and their energy consumption is only from low-frequency black/white switching when reading text or images. In the same case, our devices consume close to zero energy due to the bistability of $PProDOTMe_2$, as detailed below.

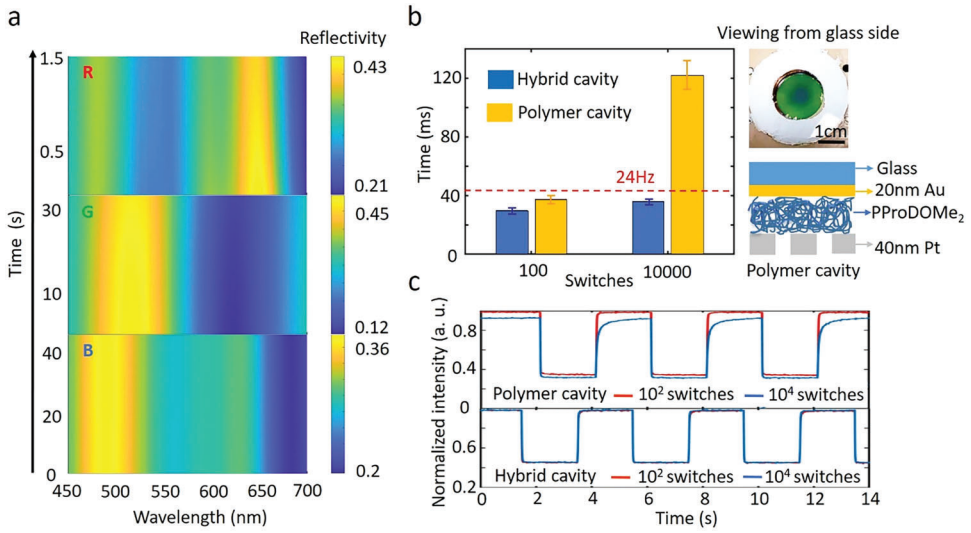

Figure 4. Characterizing bistability and lifetime. a) Temporal variation of RGB reflectivities under open circuit potential. b) Comparing switching times of hybrid and polymer cavity nanostructures (to 95% contrast), which changes with repeated switching cycles. Right: Reference sample without SiO_2 nanocaves, photograph (top) and schematic (bottom). c) Normalized reflectivities at 650 nm in time of hybrid and polymer cavity nanostructures when switching. After 10^4 switches, both the contrast and switching speed decrease for the sample without SiO_2 nanocaves.

2.4. Bistability, Lifetime, and Color Uniformity

The presented hybrid nanomaterials possess the capability for color memory (bistability), maintaining their color for a time even without applying any power, in complete contrast to emissive displays (LED, LCD). The change in RGB reflectivity vs time at open circuit potential (**Figure 4**a) shows that the fading of red is significantly faster than that of blue and green. The reflectance contrast drops by 10% after ≈1.5 s since the polymer recovers more easily from the reduced state to its equilibrium state. By contrast, it takes ≈33s for the green to lose 10% contrast, indicating that the oxidized state is more stable. The blue color is generated in the equilibrium state and so hardly fades over time. For reading text or images, the screen refresh rate can be relatively slow (>1 s). From an energy-saving perspective, our structure only needs a short-duration pulse to restore the polymer state and maintain the color before a significant fraction (e.g., 10% intensity) of the color has changed. This pulse duration should be ≈1 ms (Figure 3e), consuming ≈23 μC cm^{-2} charge. Considering the different fading times for the primary colors, red and green consume ≈8.7 and ≈0.4 μW cm^{-2} respectively, and blue does not consume any energy. These values are orders of magnitude lower than existing display devices, delivering a practically "zero" energy consumption display technology (Figure 3e).

Another important benchmark parameter is the device lifetime, which is extremely important for commercialization but rarely mentioned in tuneable color studies.[6–16,18,19,21] The nanocave structure is found to significantly improve the color uniformity of the hybrid material and prolong its lifetime. Comparing the switching speeds of nanocaves structures with those having only a polymer middle layer (Figure 4b) (using in each case samples with optimal deposition cycles, Figure S8, Supporting Information), shows that even after 10 000 switches (pulse duration 30 ms), the switching speed with nanocaves is only lengthened by ≈5 ms, and retains video rate capability. By contrast, samples with only planar polymer intracavity layers no longer support video rate after 10 000 switches, since their switching time increases from 38 to 120 ms. In addition, comparing images in Figures 4b and 2c shows that nanocave samples have better color uniformity. We attribute this to the electrochemically deposited polymers not being able to deliver uniform thickness over sufficiently large areas, leading to different Fabry–Pérot interference colors.[12] By contrast, for the nanocaves, the SiO_2 layer is deposited by physical (electron beam) evaporation with better controlled thickness. The nanocaves accommodate the polymer and simultaneously fix the distance between Au and Pt layers, ensuring color uniformity. Finally, the nanocaves protect against movement of the Pt mirror driven by polymer thickness changes during redox that can eventually lead to its collapse. Besides poorer switching speed, the optical contrast of planar samples decreases after 10 000 switches (Figure 4c), due to Pt layer partially collapse. The optical contrast of the nanocave sample exhibits no change after this number of cycles.

3. Conclusion

We have demonstrated a hybrid nanomaterial realizing a single electrochromic layer that spans RGB colors at video rate switching. The reflectance of this hybrid material is comparable to printed colors, with fourfold larger gamut coverage than state-of-the-art (static) color e-readers, while the energy consumption is lower than all existing technologies. We devised a SiO_2 nanocave structure, which allows a conjugated polymer to be in situ electrochemically deposited in a simple fashion. The reflective color is modulated by the electrochemical redox of the polymer under low (−0.6 to 0.7 V) operation voltage. We emphasize that this system achieves display of all primary colors from a single structure instead of changing the reflectivity of three different RGB subpixels. Therefore, its reflectivity is significantly improved, reaching printed color levels while retaining video display capability. This

work is thus a milestone for the E-paper industry with considerable potential.

Despite this, the system has potential for further improvement, especially in switching speed, lifetime, and chromaticity. Based on our previous research,[22] reducing the distance between working and counter-electrodes can significantly increase switching speeds. For smaller distances (≈100 µm) than here (≈2 mm), the nanocave system should deliver refresh rates easily exceeding 50 Hz. Moreover, we have proven that using ionic liquids (such as BMIM) as electrolytes extends lifetimes to $>10^7$ switches without fading.[22] Since the new hybrid nanomaterial exhibits better stability (optical contrast) in the same acetonitrile electrolyte due to fewer side reactions, this approach is promising to meet commercial requirements. We note that the exact geometry of the nanocaves should also be redesigned to match the RI changes of this electrolyte. Last, using electrochromic materials with larger optical contrast (i.e., WO_3) as the hybrid interlayer can potentially improve chromaticity. In the future, besides improving the properties, silicon solar cells (≈15 mW cm^{-2}) can be integrated into this hybrid nanomaterial. Due to its extralow power consumption, a fully self-powered display technology is thus feasible, which does not require any power source, replacing printed paper for a sustainable and scalable prospect.

4. Experimental Section

Nanofabrication: 20 nm Au and 175 nm SiO_2 were deposited by physical vapor deposition (Lesker PVD 225) using electron-gun heating. A 1 nm Cr layer was included between the Au and glass. The colloid adsorption step for generating aperiodic patterns was performed as described previously.[23] A polyelectrolyte layer was used to promote adhesion, and 300 nm polystyrene-sulphate (PS) colloids (Invitrogen) were adsorbed from a pure water suspension until saturation. Oxygen plasma at 50 W, 250 mTorr, and 80 sccm was used to shrink the particle size to 100 nm, as described previously.[32] A 1 nm Cr layer and 40 nm Pt were also deposited by physical vapor deposition using electron gun heating. The PS particles were removed by tape stripping. Samples were immersed in 0.08% hydrofluoric acid (HF) to etch the nanocaves. Then 40 nm Au and 15 nm Al_2O_3 were deposited by physical vapor deposition. The Al_2O_3 was deposited with 45° tilt and 8 rpm sample rotation.

Chemicals: Propylene carbonate and acetonitrile were purchased from Sigma. $LiClO_4$ was purchased from Fischer Scientific. The monomer (3,4-dimethylpropylenedioxythiophene) was purchased from Sycon Polymers India and purified by dispersion in deionized water (≈1 g monomer in 20 mL water) by sonication at 40 °C until a milky liquid was produced together with a brownish liquid. The milky liquid was transferred to another beaker, extracted, and recrystallized with hexane.

Electrochemical Measurements: A home-built liquid cell with Ag and Pt wires was used for three-electrode measurements. The Ag wire was chloridized prior to experiments by applying anodic potentials[25] (typically +1 V vs Pt) in 10× diluted HCl (1.16 M) in water. A potentiostat (Gamry Interface 1000) was used for electropolymerization and switching. $PProDOTMe_2$ was synthesized by linear voltage sweeps from −0.7 to 1.5 V at 200 mV s^{-1} in the presence of 0.1 M $LiClO_4$ and 0.1 M of the monomer. For color-switching measurements, the working voltage was from −0.6 to 0.75 V. Note that electrochemical deposition was in propylene carbonate for best uniformity, while the color-switching measurements were done in acetonitrile.

Optical Measurements: The chromaticity and reflectivity of the printed paper were measured by a CM-700d spectrophotometer (Konika Minolta). The colors of the PocketBook were measured in the same manner, using the device presentation document included on this e-reader, which showed circles containing the primary colors in different regions. A custom microspectroscopy setup with beamsplitters (Thorlabs) was used to measure reflectivity on the microscale in the electrochemical cell. The illumination (100 W tungsten lamp) and collection passed through a 5× air objective (NA 0.14), measured through the glass substrate into the nanostructure. Part of the reflected light was collected by an optical fiber and analyzed by a spectrometer (B&WTek CypherX). In order to get accurate absolute reflectivities, the mirror used to obtain reference intensities was also measured in the CM-700d instrument, as explained previously.[23]

Printing: The printing was done with "standard" quality settings. The three primary colors (RGB) were drawn in the Paint software of Windows 10. The red (R: 237, G: 28, B: 36) color was Hue 238, Sat 205, Lum 125, green (R: 34, G: 177, B: 76) was Hue 92, Sat 163, Lum 99, and blue (R: 0, G: 128, B: 255) was Hue 140, Sat 240, Lum 120. The printer was from HP (LaserJet Pro 400 color MFP M475dn), and also the ink cartridge (Pink: CE413, Yellow: CE412, Cyan: CE411, Black: CE410). Ordinary white A4 paper was used (Future Multitech).

Pictures and Video: The pictures and video were taken with an iPhone13 without flash. All photographs that compared colors had identical image settings, such as brightness and contrast.

Supporting Information

Supporting Information is available from the Wiley Online Library or from the author.

Acknowledgements

Lars Österlund (Uppsala University) is thanked for sharing knowledge of electrochromic devices and giving suggestions for writing this paper. Peter Andersson–Ersman (Research Institutes of Sweden) is thanked for valuable discussions about electrochemical reactions. The authors also thank Henrik Frederiksen for helping with nanofabrication. This work was financed by the Swedish Research Council (2018–06768), the Swedish Foundation for Strategic Research (EM16-0002), and UK EPSRC grants EP/L027151/1, EP/N016920/1. The authors acknowledge support from MC2 at the Chalmers University of Technology.

Conflict of Interest

The authors declare no conflict of interest.

Data Availability Statement

The data that support the findings of this study are available from the corresponding author upon reasonable request.

Keywords

electronic paper, high-reflectivity, hybrid nanocavities, video speed

Received: March 3, 2023
Revised: May 31, 2023
Published online:

[1] B. Gayral, *C. R. Phys.* **2017**, *18*, 453.
[2] L. Shao, X. Zhou, J. Wang, *Adv. Mater.* **2018**, *30*, 1704338.
[3] A. M. Chang, D. Aeschbach, J. F. Duffy, C. A. Czeisler, *Proc. Natl. Acad. Sci. USA* **2015**, *112*, 1232.

[4] B. Comiskey, J. D. Albert, H. Yoshizawa, J. Jacobson, *Nature* **1998**, *394*, 253.
[5] M. Gugole, O. Olsson, S. Rossi, M. P. Jonsson, A. Dahlin, *Nano Lett.* **2021**, *21*, 4343.
[6] D. Franklin, Y. Chen, A. Vazquez-Guardado, S. Modak, J. Boroumand, D. Xu, S. Wu, D. Chanda, *Nat. Commun.* **2015**, *6*, 7337.
[7] D. Franklin, Z. He, P. M. Ortega, A. Safaei, P. Cencillo-Abad, S.-T. Wu, D. Chanda, *Proc. Natl. Acad. Sci. USA* **2020**, *117*, 13350.
[8] R. A. Hayes, B. J. Feenstra, *Nature* **2003**, *425*, 383.
[9] B. Zhang, X. Liao, L. Xie, B. Tang, X. Zhou, H. Ye, D. Yuan, *Front. Phys.* **2022**, *10*, 3389.
[10] J. Peng, H. Jeong, Q. Lin, S. Cormier, H. Liang, M. F. L. De Volder, S. Vignolini, J. J. Baumberg, *Sci. Adv.* **2019**, *5*, eaaw2205.
[11] D. Franklin, R. Frank, S. T. Wu, D. Chanda, *Nat. Commun.* **2017**, *8*, 15209.
[12] S. Rossi, O. Olsson, S. Chen, R. Shanker, D. Banerjee, A. Dahlin, M. P. Jonsson, *Adv. Mat.* **2021**, *33*, 2105004.
[13] A. C. Arsenault, D. P. Puzzo, I. Manners, G. A. Ozin, *Nat. Photonics* **2007**, *1*, 468.
[14] G. Yang, B. Tang, D. Yuan, A. Henzen, G. Zhou, *Micromachines* **2019**, *10*, 341.
[15] E. Hopmann, A. Y. Elezzabi, *Nano Lett.* **2020**, *20*, 1876.
[16] D. P. Puzzo, A. C. Arsenault, I. Manners, G. A. Ozin, *Angew. Chem., Int. Ed.* **2009**, *48*, 943.
[17] Y. Kim, C. W. Moon, S. Kim, J. K. Hyun, *Chem. Commun.* **2022**, *58*, 12014.
[18] X. Duan, S. Kamin, N. Liu, *Nat. Commun.* **2017**, *8*, 14606.
[19] G. Wang, X. Chen, S. Liu, C. Wong, S. Chu, *ACS Nano* **2016**, *10*, 1788.
[20] D. M. Welsh, A. Kumar, E. W. Meijer, J. R. Reynolds, *Adv. Mater.* **1999**, *11*, 1379.
[21] J. Xue, Z. Zhou, Z. Wei, R. Su, J. Lai, J. Li, C. Li, T. Zhang, X. Wang, *Nat. Commun.* **2015**, *6*, 8906.
[22] K. Xiong, O. Olsson, J. Svirelis, C. Palasingh, J. Baumberg, A. Dahlin, *Adv. Mater.* **2021**, *33*, 2103217.
[23] K. Xiong, G. Emilsson, A. Maziz, X. Yang, L. Shao, E. W. H. Jager, A. B. Dahlin, *Adv. Mater.* **2016**, *28*, 10103.
[24] K. Xiong, D. Tordera, G. Emilsson, O. Olsson, U. Linderhed, M. P. Jonsson, A. B. Dahlin, *Nano Lett.* **2017**, *17*, 7033.
[25] M. Gugole, O. Olsson, K. Xiong, J. C. Blake, J. Montero Amenedo, I. Bayrak Pehlivan, G. A. Niklasson, A. Dahlin, *ACS Photonics* **2020**, *7*, 1762.
[26] J. Hwang, D. B. Tanner, I. Schwendeman, J. R. Reynolds, *Phys. Rev. B* **2003**, *67*, 115205.
[27] J. Kim, H. Oh, M. Seo, M. Lee, *ACS Photonics* **2019**, *6*, 2342.
[28] M. A. Kats, R. Blanchard, P. Genevet, F. Capasso, *Nat. Mater.* **2013**, *12*, 20.
[29] M. R. Fernandez, E. Z. Casanova, I. G. Alonso, *Sustainability* **2015**, *7*, 10854.
[30] S. V. Porter, M. Mirmehdi, B. T. Thomas, in Proc. 15th Int. Conf. on Pattern Recognition. ICPR-2000, vol. 3, IEEE, Piscataway, NJ, USA, **2000**, 409.
[31] Y. E. Lee, Y. T. Cho, Y. G. Choi, S. C. Park, M. H. Lee, Y. M. Park, D. Y. Kim, C. H. Kim, C. H. An, H. S. Kim, *Proc. IMID Dig.* **2009**, *29.2*, 360.
[32] K. Xiong, G. Emilsson, A. B. Dahlin, *Analyst* **2016**, *141*, 3803.